addition, calculational approaches may offer corroborative structural and thermodynamic evidence.[53]

Acknowledgment. We thank Dr. Michel Momenteau for very helpful discussions and Dr. Masahiro Mikuriya for experimental assistance. This work was supported by National Institutes of Health Grant GM 23851.

(53) Lopez, M. A.; Kollman, P. A. *J. Am. Chem. Soc.* **1989**, *111*, 6212.

Supplementary Material Available: Figures S1-S12 showing ^{1}H NMR spectra at 270 MHz of compounds **2-13** (12 pages). Ordering information is given on any current masthead page.

Mechanism of Halide-Induced Disproportionation of $M(CO)_3(PCy_3)_2^+$ 17-Electron Radicals (M = Fe, Ru, Os). Periodic Trends on Reactivity and the Role of Ion Pairs

Lin Song and William C. Trogler*

Contribution from the Department of Chemistry, University of California, San Diego, La Jolla, California 92093-0506. *Received June 12, 1991*

Abstract: Halide-induced disproportionation of the 17-electron $M(CO)_3(PCy_3)_2^+$ radicals was probed by double potential step chronocoulometry, rotating-ring-disk electrochemistry, bulk coulometry, and cyclic voltammetry. The products of disproportionation, $M(CO)_3(PCy_3)_2$ and $MX_2(CO)_2(PCy_3)_2$, were observed directly for M = Ru and Os, and X = Cl^- or Br^-. At a constant concentration, $[Bu_4NPF_6] + [Bu_4NX] = 0.2$ M, the kinetics of disproportionation followed the rate law $k_2[Bu_4NX][M(CO)_3(PCy_3)_2PF_6]$. Conductivity measurements in the reaction solvent CH_2Cl_2 were fit to the Fuoss equation, and K_d, the dissociation constant for the ion pairs, ranged between 2.57×10^{-5} for $[Bu_4N]Cl$ and 4.26×10^{-5} for $[Bu_4N]PF_6$ at 25 °C. The $[Fe(CO)_3(PCy_3)_2]PF_6$ species has $K_d \approx 1.7 \times 10^{-4}$. Unlike 18-electron systems, the periodic effect on the reactivity of 17-electron $M(CO)_3(PCy_3)_2^+$ showed only a slight variation. For $[Bu_4N]Cl$ at 25 °C the rates k_2 were 66 M^{-1} s^{-1} (Fe), 280 M^{-1} s^{-1} (Ru), and 27 M^{-1} s^{-1} (Os). For $[Bu_4N]Br$ hardly any variation occurred along the series: 17 M^{-1} s^{-1} (Fe), 26 M^{-1} s^{-1} (Ru), and 20 M^{-1} s^{-1} (Os). The pseudo-first-order rate constants k_{obs} showed a nonlinear dependence on the concentration of the inert electrolyte $[Bu_4N]PF_6$, and are zero order in $[Bu_4N]X$ in the absence of $[Bu_4N]PF_6$. This data, however, fit well to a kinetic scheme that involved equilibration of contact ion pairs, followed by unimolecular substitution within the contact ion pair $\{[M(CO)_3(PCy_3)_2]X\}_{ip}$. The internal substitution rates and the equilibrium constants for ion pair exchange, measured at 25 °C, are as follows (k (s^{-1}), K): for $[Bu_4N]Cl$, 15 ± 3, 0.9 ± 0.2 (Fe), 56 ± 5, 0.79 ± 0.07 (Ru), 4.8 ± 0.9, 0.7 ± 0.1 (Os); for $[Bu_4N]Br$, 3.3 ± 0.1, 0.98 ± 0.03 (Fe), 5.5 ± 0.5, 1.02 ± 0.05 (Ru), 4.4 ± 0.7, 0.9 ± 0.1 (Os). Activation parameters obtained for $M(CO)_3(PCy_3)_2^+/Bu_4NCl$ systems are as follows ($\Delta H^\ddagger$ (kcal mol^{-1}), $\Delta S^\ddagger$ (cal mol^{-1} K^{-1})): 19.7 ± 0.9, 10 ± 3 (Fe); 18.7 ± 1.6, 12 ± 5 (Ru); 12.1 ± 0.7, −14 ± 3 (Os).

Introduction

For 17-electron organometallic radicals the bulk of experimental evidence supports an associative mechanism for ligand substitution reactions.[1] A 19-electron intermediate or transition state, stabilized by metal-nucleophile σ-bonding, has been proposed[1,2] to explain the 10^9-10^{10} increase in ligand substitution rates observed[3] in comparison to analogous 18-electron complexes. One question, which remains unanswered, is the periodic effect on reactivity of 17-electron radicals. In mononuclear 18-electron complexes an enhanced reactivity occurs for second-row transition metals.[4] For example, in the iron triad[5] the relative labilities of $M(CO)_5$ complexes toward CO substitution follow the order Fe (1) < Os (800) < Ru (5×10^7). Rate data for $Fe(CO)_4(PPh_3)$[6] and $Ru(CO)_4(PPh_3)$[7] again show a 10^8 increase in reactivity for the Ru complex.

Previously we examined[3b] the disproportionation of a series of $Fe(CO)_3L_2^+$ 17-electron complexes (L = organophosphine ligand) induced by various substituted pyridine nucleophiles. This paper includes the generation of Ru and Os analogues for mechanistic comparison. Because these latter compounds are unreactive toward pyridine nucleophiles, $[NBu_4]Cl$ and $[NBu_4]Br$ nucleophiles had to be used for the complete triad. Halide ions were known[8] to cause disproportionation for $Fe(CO)_3(PPh_3)_2^+$. An additional interesting question about the role of ion pairs vs free ions arose in the study of this reaction mechanism. Ion pairing of charged organometallic compounds has been observed spectroscopically for many systems in solvents of low dielectric constant.[9,10] The most common examples involve salts of carbonylmetalates. For example, Kochi's work[10] clearly establishes the importance of contact ion pair equilibria on the photochemistry of organometallic charge-transfer complexes. The study described here for carbonylmetal cations suggests a crucial role for ion pairing in their

(1) (a) Tyler, D. R. *Prog. Inorg. Chem.* **1988**, *36*, 125. (b) Trogler, W. C. In *Organometallic Radical Processes*; Trogler, W. C., Ed.; Elsevier: Amsterdam, 1990; pp 306-337.
(2) Therien, M. J.; Trogler, W. C. *J. Am. Chem. Soc.* **1988**, *110*, 4942.
(3) (a) Shi, Q.-Z.; Richmond, T. G.; Trogler, W. C.; Basolo, F. *J. Am. Chem. Soc.* **1984**, *106*, 71. (b) Therien, M. J.; Ni, C.-L.; Anson, F. C.; Osteryoung, J. G.; Trogler, W. C. *J. Am. Chem. Soc.* **1986**, *108*, 4037.
(4) (a) Basolo, F.; Pearson, R. C. *Mechanisms of Inorganic Reactions*, 2nd ed.; Wiley: New York, 1967; p 576. (b) Atwood, J. D. *Inorganic and Organometallic Reaction Mechanisms*; Brooks/Cole Publ.: Monterey, CA, 1985; pp 108-111.
(5) Shen, J.-K.; Gao, Y.-C.; Shi, Q.-Z.; Basolo, F. *Inorg. Chem.* **1989**, *28*, 4304.
(6) Siefert, E. E.; Angelici, R. J. *J. Organomet. Chem.* **1967**, *8*, 374.
(7) Johnson, B. F. G.; Lewis, J.; Twigg, M. V. *J. Chem. Soc., Dalton Trans.* **1975**, 1876.
(8) Baker, P. K.; Connelly, N. G.; Jones, B. M. R.; Maher, J. P.; Somers, K. R. *J. Chem. Soc., Dalton Trans.* **1980**, 579.
(9) Darensbourg, M. Y.; Ash, C. E. *Adv. Organomet. Chem.* **1987**, *27*, 1.
(10) Kochi, J. K. In *Organometallic Radical Processes*; Trogler, W. C., Ed.; Elsevier: Amsterdam, 1990; pp 201-269.

0002-7863/92/1514-3355$03.00/0

reactions with charged nucleophiles.

Experimental Section

Materials. Iron pentacarbonyl (Strem), tricyclohexylphosphine (Strem), ruthenium(III) chloride hydrate (Strem), and osmium tetraoxide (Aldrich) were used as received. Solvents were distilled under a nitrogen atmosphere. Methylene chloride was refluxed over CaH_2; THF, pentane, and diethyl ether were dried over sodium benzophenone ketyl. $Fe(CO)_3(PCy_3)_2$ was synthesized photochemically from iron pentacarbonyl and tricyclohexylphosphine.[11] Ammonium hexabromoosmate was prepared by the method of Dwyer and Hogarth.[12]

Synthesis of $Ru(CO)_3(PCy_3)_2$. This complex was prepared by a method similar to that reported for the synthesis of $Ru(CO)_3(PPh_3)_2$.[13] Solutions of 0.39 g (15 mmol) of hydrated ruthenium trichloride in 30 mL of cool 2-methoxyethanol, hot aqueous formaldehyde (33 mL, 37 wt %), and 0.6 g of KOH in 30 mL of hot 2-methoxyethanol were added rapidly and successively to a well-stirred boiling solution of 2.52 g (9 mmol) of tricyclohexylphosphine in 90 mL of 2-methoxyethanol under nitrogen. The reaction solution was heated under reflux overnight, and then cooled to room temperature. The resulting pale-yellow precipitate was washed with ethanol, water, ethanol, and hexane, and then dried in vacuum. Yield: 0.95 g (85%). Anal. Calcd for $C_{39}H_{60}P_2O_3Ru$: C, 62.79; H, 8.92. Found: C, 62.32; H, 8.92.

Synthesis of $OsBr_2(CO)_2(PCy_3)_2$. This compound was prepared similar to a method of Collman and Roper[14] reported for $OsBr_2(CO)_2(PPh_3)_2$. $(NH_4)_2OsBr_6$ (0.7 g) was suspended in 60 mL of 2-methoxyethanol in a Fischer-Porter glass pressure bottle. After stirring and heating at 80 °C under 50 psi of CO for 1 or 2 days, a clear pale-yellow solution was obtained. The bottle was vented, 1.0 g of tricyclohexylphosphine was added, and the solution was heated at 80 °C and stirred for another hour. Some pale-yellow $OsBr_2(CO)_2(PCy_3)_2$ precipitated, and cooling the mixture in an ice bath yielded 0.6 g (62%) of the desired product. Its infrared spectrum in CH_2Cl_2 shows absorptions at 2012 and 1939 cm^{-1} similar to those reported for the PPh_3 derivative at 2035 and 1970 cm^{-1}.[14]

Synthesis of $Os(CO)_3(PCy_3)_2$. $OsBr_2(CO)_2(PCy_3)_2$ (0.5 g) was suspended in 15 mL of THF, and CO was bubbled through the suspension for 10 min. The bubbling was continued as a slurry of 1.5 g of potassium graphite (C_8K)[15] in 15 mL of THF was added slowly with stirring. An excess of C_8K was required before the infrared spectra showed no more $OsBr_2(CO)_2(PCy_3)_2$ present in the solution. The reaction mixture was then filtered under nitrogen. The pale-yellow filtrate was concentrated to about 5 mL, and 20 mL of methanol was added. The crystalline precipitate was washed with ether and then dried under vacuo (0.17 g, 40%). Anal. Calcd for $C_{39}H_{66}P_2O_3Os$: C, 56.09; H, 7.97. Found: C, 55.69; H, 8.40.

Conductivity Measurements. The thermostated conductivity cell had a cell constant of 0.107 ± 0.001 cm^{-1}, which was determined with an aqueous KCl reference solution.[16] The conductivity was measured with a Yellow Springs Instrument Co. Model 31 conductivity bridge. Solutions in the range of 7×10^{-6} to 2×10^{-4} M were made by diluting 1.5×10^{-3} M stock solutions. A complete series of measurements for a compound at one temperature consisted of 12–14 measurements of the equivalent conductivity as a function of concentration.

Electrochemical Studies. The supporting electrolyte tetra-*n*-butylammonium hexafluorophosphate (Southwestern Chemical) was recrystallized from a mixture of ethyl acetate and pentane and dried in vacuo. Tetra-*n*-butylammonium chloride (Kodak) was recrystallized from dry acetone and ether and dried in vacuo for 2 days. Tetra-*n*-butylammonium bromide (GFS Chemicals) was used as received.

Both cyclic voltammetry (CV) and double potential step chronocoulometry (DPSCC) measurements were carried out under N_2 with a BAS-100 electrochemical analyzer. A J-shaped platinum working electrode with about a 0.2 mm^2 surface area, a platinum wire auxiliary electrode, and a silver wire reference electrode were employed for the experiments. No IR compensation was used, and the analysis of Q vs $t^{1/2}$ plots showed that capacitative charging effects did not affect the charge ratios appreciably (<5%) over the range of pulse widths used in the analysis. A rotating-ring-disk electrode (RRDE) was used with a EG&G PARC Model 366 bipotentiostat and an IBM 7424 *X–Y* recorder. A Ag/0.1 M $AgNO_3$ reference electrode (in CH_3CN) was separated from the test solution by a glass jacket with a porous Vycor tip, in order to avoid leakage of Ag^+ ions into the solution. A blanket of nitrogen, which was presaturated with solvent by passing it through two solvent saturators, was maintained in the electrochemical cell by continuous purging.

Digital simulation of proposed electrochemical mechanisms was done by the Feldberg digital simulation method to generate working curves other than those reported by Reilly et al.[17]

Spectral Studies. Infrared spectra were recorded by using an IBM FTIR/32. Electron paramagnetic resonance (EPR) spectra were recorded at room temperature and at 77 K with a Varian E-3 spectrometer, and external diphenylpicrylhydrazyl was used as the field marker.

Elemental Analyses. Microanalysis was carried out on a Perkin-Elmer 2400 CHN elemental analyzer at the Scripps Institute of Oceanography Analytical Facility.

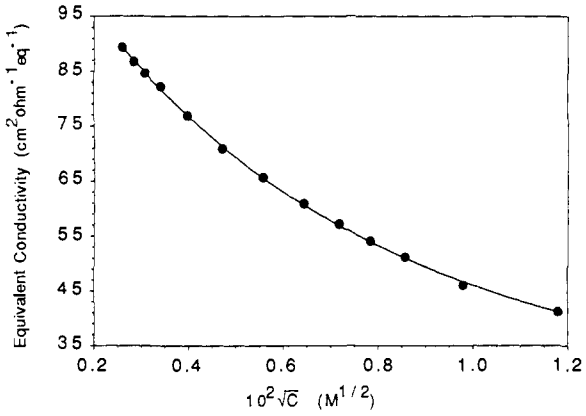

Figure 1. Equivalent conductivity of tetrabutylammonium chloride as a function of concentration: (●) experimental data; (—) calculated least-squares line from fitting to the Fuoss equation.

Table I. Dissociation Constants from Conductivity Measurements[a,b]

compound	Λ_0, cm^2 Ω^{-1} $equiv^{-1}$	$K_d \times 10^5$
$[Bu_4N]Cl$	109 (±1)	2.57[f]
$[Bu_4N]Cl$[c]	104 (±2)	2.92
$[Bu_4N]Cl$[d]	91 (±1)	4.15
$[Bu_4N]Cl$[e]	82 (±1)	4.94
$[Bu_4N]Br$	112 (±1)	2.71
$[Bu_4N]I$	121 (±2)	3.57
$[Bu_4N]PF_6$	121 (±2)	4.26
$[Bu_4N]PF_6$[c]	110 (±2)	4.66
$[Bu_4N]PF_6$[d]	99 (±2)	5.40
$[Bu_4N]PF_6$[e]	91 (±2)	5.62
$[Bu_4N]ClO_4$	118 (±1)	3.37
$[Fe(CO)_3(PCy_3)_2]PF_6$	95 (±1)	16.6

[a] Measured in methylene chloride. Solvent dielectric constant and viscosities (cP): 8.93, 0.39. Errors in K_d are within 10%. [b] At 25.0 °C unless otherwise indicated. [c] At 10.0 °C. [d] At 0.0 °C. [e] At −10.0 °C. [f] $K_d = 2.44 \times 10^{-5}$ ($K_a = 4.1 \times 10^4$) as previously reported.[19]

Table II. Thermodynamic Parameters for Ion Pair Dissociation

compound	ΔH, kcal mol^{-1}	ΔS, cal mol^{-1} K^{-1}
$[Bu_4N]Cl$	−3.1 (±0.7)	−31 (±7)
$[Bu_4N]PF_6$	−1.3 (±0.3)	−24 (±5)

Results and Discussion

Ion Pair Dissociation Constants from Conductivity Measurements. The conductivity data in CH_2Cl_2 for various one-to-one highly associated electrolytes were fit to the Fuoss equation[18] to obtain dissociation constants. The computer-fitting program used an IBM 9000 computer and was based on that of Fuoss.[18] Only the limiting conductance (Λ_0) and the dissociation constant were treated as adjustable parameters to minimize σ^2, and the radius

(11) Therien, M. J.; Trogler, W. C. *Inorg. Synth.* **1989**, *25*, 151.
(12) Dwyer, F. P.; Hogarth, J. W. *Inorg. Synth.* **1957**, *5*, 204.
(13) Ahmad, N.; Levison, J. J.; Robinson, S. D.; Uttley, M. F. *Inorg. Synth.* **1974**, *15*, 50.
(14) Collman, J. P.; Roper, W. R. *J. Am. Chem. Soc.* **1967**, *88*, 3504.
(15) Schwindt, M. A.; Lejon, T.; Hegedus, L. S. *Organometallics* **1990**, *9*, 2814.
(16) Lind, J. E.; Zwolenik, J. J.; Fuoss, R. M. *J. Am. Chem. Soc.* **1959**, *81*, 1557.
(17) Hanafey, M. K.; Scott, R. L.; Reilley, C. N. *Anal. Chem.* **1978**, *50*, 116.
(18) Fuoss, R. M. *J. Phys. Chem.* **1978**, *82*, 2427.

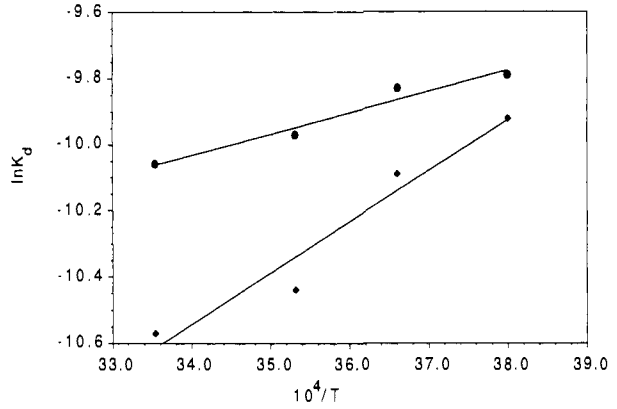

Figure 2. van't Hoff plots of K_d for tetrabutylammonium chloride (◆) and tetrabutylammonium hexafluorophosphate (●).

parameter (R) was optimized by setting it equal to a known or suggested value (e.g., 29 Å for $[Bu_4N]Cl$ as reported by Balt and Tieleman,[19] 35–45 Å for $[Bu_4N]PF_6$). The fitting was not really sensitive to R, as was also observed by Fuoss.[18] An example shown in Figure 1 illustrates the excellent agreement between experimental and calculated values of the conductivity for $[Bu_4N]Cl$ at 25.0 °C. The results of these fits are shown in Table I. The 17-electron $[Fe(CO)_3(PCy_3)_2][PF_6]$ complex was stable enough for solution conductivity measurements under a nitrogen atmosphere in the dark. The ion pair dissociation constant determined is similar to those found for salts of 18-electron organometallic cations in THF.[20] For two compounds in Table I, $[Bu_4N]Cl$ and $[Bu_4N][PF_6]$, the temperature dependence of K_d was determined by recording measurements at four different temperatures (−10.0, 0, 10.0, and 25.0 °C). The van't Hoff plots of K_d as a function of temperature are shown in Figure 2. The parameters obtained from the plots are summarized in Table II.

As can be seen in Table I lowering the temperature increases K_d for $[Bu_4N]Cl$ and $[Bu_4N][PF_6]$. This resembles a previous report[19] that the K_a ($1/K_d$) for $[Et_4N][FeCl_4]$ in CH_2Cl_2 decreases as the temperature is lowered. Therefore, dissociation of the ion pair is exothermic (Table II). The small value for K_d must therefore result from the unfavorable (negative) entropic term (Table II). This is consistent with the separated ions being more strongly solvated than the ion pair. The entropy loss associated with ordering of the solvent around the free ions must dominate over the entropy gain expected for dissociation of the ion pair into its two components.

Characterization and Electrochemical Studies of the Disproportionation Reactions. The $[Fe(CO)_3(PCy_3)_2][PF_6]$ complex can be isolated by oxidation of neutral $Fe(CO)_3(PCy_3)_2$ with 1 equiv of $[(4\text{-}BrC_6H_5)_3N][PF_6]$ in CH_2Cl_2.[3b] The analogous Ru(I) compound can be generated from $Ru(CO)_3(PCy_3)_2$ with 1 equiv of $[(4\text{-}BrC_6H_5)_3N][PF_6]$ or $AgPF_6$ in CH_2Cl_2 at 0 °C. Its infrared spectrum taken immediately after the preparation shows a sharp band at 1993 cm^{-1} and two weak bands at 2027 and 2060 cm^{-1}. The room temperature EPR solution spectrum shows a feature at $g = 2.051$. The light brown solution quickly loses color, and the infrared spectrum taken $^1/_2$ h later shows the two peaks at 2027 and 2060 cm^{-1} with increased intensity. The 1993-cm^{-1} absorption disappeared completely. Because of the similarity to the Fe(I) complex, we attribute the 1993-cm^{-1} absorption and $g = 2.051$ feature to highly reactive $[Ru(CO)_3(PCy_3)_2][PF_6]$, which perhaps forms $[Ru(CO)_3(PCy_3)_2Cl][PF_6]$, on standing as reported by Gladfelter et al.[21] for $[Ru(CO)_3(PPh_3)_2Cl][PF_6]$.

The light-brown product initially obtained from oxidation of $Os(CO)_3(PCy_3)_2$ with 1 equiv of $AgPF_6$ appears to be unstable. The solution turned pale yellow before its infrared spectrum could be recorded. Three absorptions at 1921 (s), 2004 (w), and 2044 (w) are obtained, and no further change is observed in a 5-h time period. The EPR signal of the solution is weak and noisy, but consistent with the presence of $Os(CO)_3(PCy_3)_2^+$ in small amounts. The results from CV, IR, and EPR studies are listed in Table III.

Initial electrochemical studies of $M(CO)_3(PCy_3)_2$ (M = Fe, Ru, Os) by cyclic voltammetry revealed reversible to quasireversible behavior. Qualitative studies of the halide-induced disproportionation reactions were performed by adding known concentrations of halide to a solution of $M(CO)_3(PCy_3)_2$ in CH_2Cl_2. Disappearance of the reduction peaks could be observed for all three complexes, as seen in the matrix of cyclic voltammograms (Figure 3). Disproportionation, which occurs on addition of tetra-*n*-butylammonium chloride or bromide, was evidenced by the appearance of both $M(CO)_3(PCy_3)_2$ and $MX_2(CO)_2(PCy_3)_2$ in the IR spectra.

A study of the reaction stoichiometry was carried out by generating $[M(CO)_3(PCy_3)_2]PF_6$ quantitatively through bulk electrolysis, followed by measuring the characteristic IR absorbance of neutral $M(CO)_3(PCy_3)_2$, which appeared immediately after addition of 10 equiv of the halide species. Using the measured IR extinction coefficients of $M(CO)_3(PCy_3)_2$ (M = Fe, $\epsilon = 1.2 \times 10^3$ M^{-1} cm^{-1}; M = Ru, $\epsilon = 8.9 \times 10^2$ M^{-1} cm^{-1}; M = Os, $\epsilon = 1.0 \times 10^3$ M^{-1} cm^{-1}), it was found that about 0.80–1.02 mol of $Fe(CO)_3(PCy_3)_2$ or $Ru(CO)_3(PCy_3)_2$ forms for every 2 mol of the corresponding cationic radical that reacts. Only small amounts (0.1–0.2 mol) of $Os(CO)_3(PCy_3)_2$ were observed in the IR spectrum, because of the instability of $[Os(CO)_3(PCy_3)_2][PF_6]$ radical. The stoichiometry of the reaction between $Os(CO)_3(PCy_3)_2^+$ and halide could, however, be characterized by conducting bulk electrolysis in the presence of halide. With 20 equiv

Table III. Cyclic Voltammetric, Infrared, and Electron Paramagnetic Resonance Spectral Data for $M(CO)_3L_2^+$ Complexes in CH_2Cl_2

complex	$E_{1/2}$,[a] V	ΔE_p,[a] V	18e ν_{CO}, cm^{-1}	17e ν_{CO}, cm^{-1}	$\langle g \rangle$
$Fe(CO)_3(PCy_3)_2^{0/+}$	0.37	0.12	1846	1973	2.056
$Ru(CO)_3(PCy_3)_2^{0/+}$	0.25	0.07	1856	1993[b]	2.051
$Os(CO)_3(PCy_3)_2^{0/+}$	0.32	0.10	1848	*c*	2.053

[a] Experimental conditions: $[M(CO)_3(PCy_3)_2] = 1.0 \times 10^{-3}$ M; supporting electrolyte 0.2 M tetrabutylammonium hexafluorophosphate; temperature 23 ± 2 °C, scan rate 200 mV/s; solvent CH_2Cl_2; platinum working electrode, platinum wire auxiliary electrode, and Ag wire reference electrode used for the measurements. The ferrocene oxidation potential under these conditions was 0.84 V. [b] 1991 cm^{-1} reported by Gladfelter et al.[21] [c] The 17-electron complex was unstable to decomposition in the time required to obtain an IR spectrum to form a species with ν_{CO} at 1921 (s), 2004 (w), and 2044 (w) cm^{-1}.

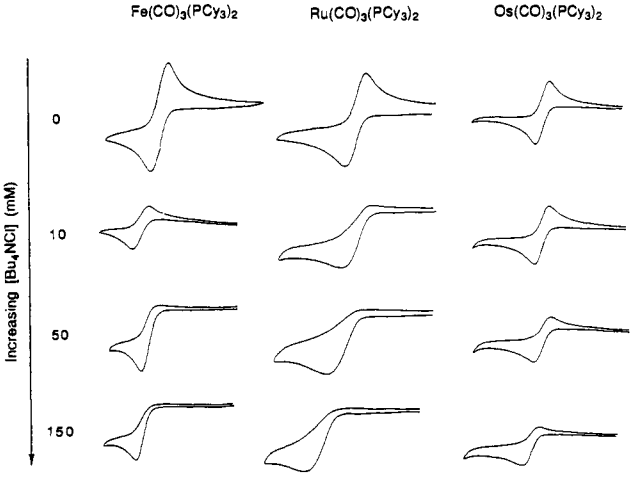

Figure 3. A matrix of cyclic voltammograms of $M(CO)_3(PCy_3)_2$ (M = Fe, Ru, Os) at varying concentrations of tetrabutylammonium chloride at a fixed scan rate. Experimental conditions: $[M(CO)_3(PCy_3)_2] = 1 \times 10^{-3}$ M, $[Bu_4NPF_6] = 0.2$ M, scan rate 200 mV/s, temperature 23 ± 2 °C, solvent CH_2Cl_2, no IR compensation used.

(19) Balt, S.; du Chattel, G.; de Kieviet, W.; Tieleman, A. *Z. Naturforsch., B: Anorg. Chem., Org. Chem.* **1978**, *33B*, 745.
(20) Darensbourg, M.; Borman, C. *Inorg. Chem.* **1976**, *15*, 3121.
(21) Sherlock, S. J.; Boyd, D. C.; Moasser, B.; Gladfelter, W. L. *Inorg. Chem.* **1991**, *30*, 3626.

Table IV. Results from Controlled-Potential Bulk Electrolysis of $M(CO)_3(PCy_3)_2$ with and without $[Bu_4N]X$ in CH_2Cl_2 Solution (M = Fe, Ru, Os; X = Cl, Br)[a]

compound	n [Bu_4NX] = 0 equiv	n [Bu_4NCl] = 20 equiv	ν_{CO} of product, cm^{-1}	n [Bu_4NBr] = 20 equiv	ν_{CO} of product, cm^{-1}
$Fe(CO)_3(PCy_3)_2$	0.90	2.65	none observed[b]	3.57	none observed
$Ru(CO)_3(PCy_3)_2$	0.89	1.41	1962, 2029	1.51	1964, 2031
$Os(CO)_3(PCy_3)_2$	0.95	1.56	1943, 2018	1.65	1939, 2014

[a] Experimental conditions: Supporting electrolyte 0.1 M $[Bu_4N]PF_6$, temperature 23 ± 2 °C, $M(CO)_3(PCy_3)_2$ oxidized on the surface of platinum gauze with platinum wire as auxiliary electrode and a silver wire as reference electrode. The electrodes are placed in three compartments separated by fritted glass disks. The errors for the measurements are 10–20%. [b] Further oxidation of $FeCl_2(CO)_2(PCy_3)_2$, which could be detected as an intermediate, occurred (see text).

of tetra-*n*-butylammonium chloride or bromide present in the solution, $OsX_2(CO)_2(PCy_3)_2$ product was observed in the IR spectra. Only a net one-electron oxidation occurred at the same potential when no halide was added. It appears that $Os(CO)_3(PCy_3)_2^+$, once generated at the surface of electrode, reacts immediately with halide to generate an intermediate, which disproportionates to $OsX_2(CO)_2(PCy_3)_2$ and $Os(CO)_3(PCy_3)_2$. The latter species is oxidized to undergo further disproportionation, and the process continues until all Os(0) complex is exhausted to provide $OsX_2(CO)_2(PCy_3)_2$ as the final product. We observed similar behavior with $Ru(CO)_3(PCy_3)_2$, which underwent a two-electron oxidation when halide was present to form $RuX_2(CO)_2(PCy_3)_2$. For iron the apparent instability of $FeX_2(CO)_2(PCy_3)_2$ led to more complex behavior, since a greater than two-electron oxidation occurs on bulk electrolysis. However, an infrared spectrum obtained by quickly mixing cold solutions of $[Fe(CO)_3(PCy_3)_2][PF_6]$ and an excess amount of tetra-*n*-butylammonium chloride in CH_2Cl_2 shows two weak absorptions attributable to $FeCl_2(CO)_2(PCy_3)_2$ at 1956 and 2013 cm^{-1}, in addition to a strong absorption band of $Fe(CO)_3(PCy_3)_2$ at 1846 cm^{-1}. The weak absorptions disappeared within 5 min, which is consistent with an unstable $FeX_2(CO)_2(PCy_3)_2$ species. The results from these experiments are summarized in Table IV. The bulk electrolysis data generally show nonideal *n* values, which reflect the possible importance of side reactions under conditions of exhaustive electrolysis.

Kinetics of the Disproportionation Reactions. The double potential step chronocoulometric method[17,22] was employed to measure the reaction rate of the halide-induced disproportionation. Although those 17-electron radicals showed various degrees of instability in CH_2Cl_2 over a relatively long period of time (minutes), their charge ratios obtained by DPSCC (Q_r/Q_f = 0.580 for $Fe(CO)_3(PCy_3)_2^+$; 0.590 for $Ru(CO)_3(PCy_3)_2^+$; 0.589 for $Os(CO)_3(PCy_3)_2^+$ at pulse widths as long as 1 s) were very close to the expected value of 0.586 for a chemically reversible reaction. This makes the systems suitable for kinetic studies by using the transient electrochemical technique DPSCC. Charge ratios (Q_r/Q_f) deviated from reversible behavior when halide was added to the solution. When the pulse widths τ and concentration of halide were varied, the Q_r/Q_f data could be fit to working curves of mechanisms that could yield the products established by previous infrared and electrochemical studies. As an example, the working curve for the EC half-regeneration mechanism and the experimental data for the reaction between $[Fe(CO)_3(PCy_3)_2]PF_6$ and 0.200 M $[Bu_4N]Cl$ at 15 °C are shown in Figure 4.

Although we considered more elaborate mechanisms by digital simulation techniques, the best fits always reduced to the limiting case where $M(CO)_3L_2^+$ initially reacts by a process first order in halide (Figure 5), and where the ensuing steps occur rapidly. Rate constants determined for the EC half-regeneration mechanism (Scheme I) are listed in Table V. We refer to the rate constants in Table V as pseudo-second-order rates (k_2). The bulk

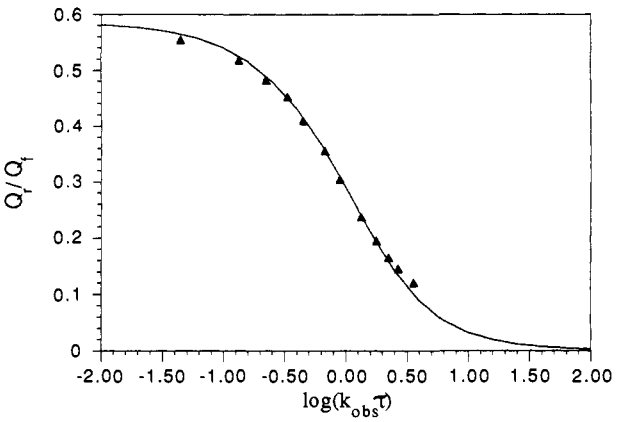

Figure 4. Charge ratios (Q_r/Q_f) as a function of log ($k_{obs}\tau$) for the EC half-regeneration mechanism: (—) working curve; (▲) experimental data of $Fe(CO)_3(PCy_3)_2^+$ with 0.200 M $[Bu_4N]Cl$ at 15 °C ($[Bu_4NPF_6]$ = 0).

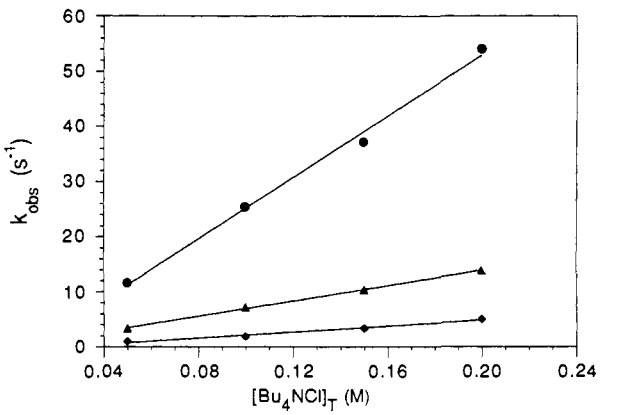

Figure 5. Observed pseudo-first-order rate constant as a function of the total concentration of $[Bu_4N]Cl$ for the reaction between $M(CO)_3(PCy_3)_2^+$ and $[Bu_4N]Cl$, measured at $[Bu_4NCl] + [Bu_4NPF_6] = 0.2$ M: (●) M = Ru; (▲) M = Fe; (◆) M = Os.

Table V. Pseudo-Second-Order Rate Constants for Halide-Induced Disproportionation of $M(CO)_3(PCy_3)_2^+$ in CH_2Cl_2 at 25.0 °C[a]

radical	halide	DPSCC k_2, M^{-1} s^{-1}	RRDE k_2, M^{-1} s^{-1} [b]
$Fe(CO)_3(PCy_3)_2^+$	$[Bu_4N]Cl$	66 (±6)	70 (±3)
$Fe(CO)_3(PCy_3)_2^+$	$[Bu_4N]Br$	17 (±2)	21 (±2)
$Ru(CO)_3(PCy_3)_2^+$	$[Bu_4N]Cl$	280 (±22)	302 (±16)
$Ru(CO)_3(PCy_3)_2^+$	$[Bu_4N]Br$	26 (±3)	20 (±1)
$Os(CO)_3(PCy_3)_2^+$	$[Bu_4N]Cl$	27 (±4)	26 (±3)
$Os(CO)_3(PCy_3)_2^+$	$[Bu_4N]Br$	20 (±3)	13 (±2)

[a] Reaction rates were measured at constant ionic strength, $[Bu_4NX]_T + [Bu_4NPF_6]_T = 0.2$ M. [b] The errors for the RRDE reflect the consistency in a series of measurements. Systematic errors from estimating the limiting current or from solvent loss in a dynamically purged system are such that we estimate a 20% uncertainty as a more realistic value.

(22) (a) Christie, J. H.; Anson, F. C.; Lauer, G.; Osteryoung, R. A. *Anal. Chem.* **1963**, *35*, 1979. (b) Bard, A. J.; Faulkner, L. R. *Electrochemical Methods*; Wiley: New York, 1980. (c) Christie, J. H.; Osteryoung, R. A.; Anson, F. C. *J. Electroanal. Chem. Interfacial Electrochem.* **1967**, *13*, 236. (d) Christie, J. H. *Ibid.* **1967**, *13*, 73. (e) Anson, F. C. *Acc. Chem. Res.* **1975**, *8*, 400 and references therein.

Table VI. $[Bu_4NCl]_{ip}$ and $[Cl^-]_{free}$ Calculated from the Measured K_d of Bu_4NCl and Bu_4NPF_6 under Various Experimental Conditions in CH_2Cl_2

$[Bu_4NCl]_T$	$[Bu_4NPF_6]_T$	$[Bu_4NCl]_{ip}$	$[Cl^-]_{free}$
0.0500[a]	0.150	0.0495	0.000462
0.100[a]	0.100	0.0990	0.000982
0.150[a]	0.050	0.148	0.00157
0.200[a]	0	0.198	0.00226
0.0500[b]	0.150	0.0495	0.000501
0.0100[b]	0.100	0.0989	0.00106
0.150[b]	0.050	0.148	0.00168
0.200[b]	0	0.198	0.00240
0.0500[c]	0.150	0.0494	0.000647
0.100[c]	0.100	0.0987	0.00134
0.150[c]	0.050	0.148	0.00208
0.200[c]	0	0.197	0.00286

[a] At 25 °C. [b] At 10.0 °C. [c] At 0 °C.

coulometry experiments and product analysis have already shown that about $^1/_2$ mol of $M(CO)_3L_2$ is regenerated for each mole of $M(CO)_3L_2^+$, which undergoes disproportionation for M = Ru and Os. For the iron analogue we assume similar behavior at the short times of the kinetics experiments, although bulk coulometry and the spectroscopic measurements suggest the instability of $FeX_2(CO)_2(PCy_3)_2$ ultimately leads to oxidation with the production of Fe^{3+}.

Scheme I. EC Half-Regeneration Mechanism

$$M(CO)_3L_2 \underset{E_f}{\overset{E_i}{\rightleftharpoons}} M(CO)_3L_2^+ + e$$

$$M(CO)_3L_2^+ + [Bu_4N]X \xrightarrow{k_2} {}^1/_2M(CO)_3L_2 + {}^1/_2MX_2(CO)_2L_2 + CO$$

Rotating-ring-disk electrode experiments (RRDE) on the same systems were carried out, and collection efficiencies were obtained at different rotation speeds. The diffusion constants were first measured in the absence of nucleophile by fitting the limiting current data to the Levich equation. The measured diffusion coefficients at 25.0 °C were 6.46×10^{-6} cm^2/s for $Fe(CO)_3(PCy_3)_2$, 4.78×10^{-6} cm^2/s for $Ru(CO)_3(PCy_3)_2$, and 5.51×10^{-6} cm^2/s for $Os(CO)_3(PCy_3)_2$. Rate constants for a first-order intervening reaction mechanism (Scheme II) could then be determined from measured collection efficiencies according to equations derived by Albery and Hitchman.[23] The pseudo-second-order rate constants determined by RRDE experiments are also shown in Table V.

Scheme II

$$\text{disk:}\quad M(CO)_3L_2 \rightarrow M(CO)_3L_2^+ + e$$

$$\text{solution:}\quad M(CO)_3L_2^+ + Bu_4X \xrightarrow{k_2} \text{products}$$

$$\text{ring:}\quad M(CO)_3L_2^+ + e \rightarrow M(CO)_3L_2$$

These measurements provide an independent check on the EC half-regeneration mechanism we assumed in the analysis of the double potential step experiments. In the RRDE measurements the effects of half-regeneration in the disproportionation step are diminished, because the formation of $M(CO)_3L_2$ does not effect the cathodic current at the ring. Although the RRDE experiments are more prone to error, because of the inherent difficulty involved in applications to air-sensitive compounds and the need to estimate limiting currents, they provide a more direct measure of the rate constant involved in the decay of $M(CO)_3L_2^+$. The rates (Table V) measured by the RRDE method all agree with the DPSCC values to within three standard deviations of the measurements.

Ion Pair Reactivity. The ion pair dissociation constants (K_d) derived in the analysis of conductivity data assume the limit of infinite dilution and near-zero ionic strength. The dependence of the K_d's on ionic strength can be estimated according to the theoretical equation derived independently by Fuoss and Eigen.[24]

(23) Albery, W. J.; Hitchman, M. L. *Ring-Disc Electrodes*; Oxford University Press: London, 1971; pp 122–133.

Table VII. Observed Pseudo-First-Order Rate Constants for the Reaction between $Ru(CO)_3(PCy_3)_2^+$ and Bu_4NCl Measured at 25.0 °C in CH_2Cl_2[a]

$[Bu_4NCl]_T$	$[Bu_4NPF_6]_T$	k_{obs}, s^{-1}	$[Bu_4NCl]_T$	$[Bu_4NPF_6]_T$	k_{obs}, s^{-1}
0.050	0	57	0.100	0.200	16
0.050	0.150	12	0.150	0	56
0.100	0	60	0.150	0.05	37
0.100	0.100	26	0.200	0	54

[a] Errors in k_{obs} are within 10%.

It has been reported that K_d ($1/K_A$) increases by a factor of 10–100 in polar solvents, such as water and methanol, as the ionic strength varies from 0 to 0.500 M.[25] However, our calculations for CH_2Cl_2 solvent show that ion pairs do not dissociate appreciably under the experimental conditions, which is consistent with the results reported in other nonpolar solvents such as bromobenzene and chloroform.[26] The highly associated $[Bu_4N]X$ and $[Bu_4N][PF_6]$ electrolytes contribute little to the change of ionic strength. We calculate that the K_d's do not deviate significantly (<15%) from those measured at near-zero ionic strength. Because the theoretical estimate can only be considered reliable to a factor of 5–10, we did not include this small correction. Concentrations of $[Bu_4N]X$ ion pairs, $[Bu_4NX]_{ip}$, and X^- free ion, $[X^-]_{free}$ (X = Cl, Br), under various experimental conditions could be calculated from the measured dissociation constants of $[Bu_4N]X$ and $[Bu_4N][PF_6]$ (Table VI). A plot of the pseudo-first-order rate constants (k_{obs}) vs $[Bu_4NX]_{ip}$ is essentially indistinguishable from Figure 5. As $k_{obs} = k_{ip}[Bu_4NX]_{ip} + k_{free}[X^-]_{free}$, the excellent linear plots of k_{obs} vs $[Bu_4NX]_{ip}$ imply $k_{free}[X^-]_{free} \approx 0$. Although this initially suggested that $[Bu_4NX]_{ip}$ behaved as the nucleophile, this picture is too simplistic.

Ionic Strength or Inert Salt Effects. We have observed strong effects on the pseudo-first-order rate constants for disproportionation of $M(CO)_3(PCy_3)_2^+$ with halide on addition of the inert salt $[Bu_4N][PF_6]$. With constant $[Bu_4NX]$, the rate constants decreased as the supporting electrolyte $[Bu_4N][PF_6]$ concentration increased. However, in the absence of $[Bu_4N][PF_6]$ no significant change in reaction rates was observed with different amounts of $[Bu_4N]X$ present in the solution (an example for the $Ru(CO)_3(PCy_3)_2^+/Bu_4NCl$ system is shown in Table VII). Thus, the reaction appeared to be first order in $[Bu_4N]Cl$ if $[Bu_4N][PF_6]$ was the supporting electrolyte; however, zero-order behavior in $[Bu_4N]Cl$ was obtained when no $[Bu_4N][PF_6]$ electrolyte was added! We therefore explored a new kinetic scheme, which involved preequilibration of ion pairs, followed by unimolecular substitution within the contact ion pair $[M(CO)_3(PCy_3)_2X]_{ip}$ (Scheme III), followed by rapid electron transfer to yield the ultimate products. Assuming $[Bu_4NPF_6]_{ip} \gg [M(CO)_3L_2X]_{ip}$

Scheme III

$$[M(CO)_3L_2PF_6]_{ip} + [Bu_4NX]_{ip} \underset{}{\overset{K}{\rightleftharpoons}} [M(CO)_3L_2X]_{ip} + [Bu_4NPF_6]_{ip}$$

$$[M(CO)_3L_2X]_{ip} \xrightarrow{k} {}^1/_2M(CO)_3L_2 + {}^1/_2M(CO)_2L_2X_2 + CO$$

and $[Bu_4NX]_{ip} \gg [M(CO)_3L_2X]_{ip}$, $[M(CO)_3L_2^+]_T = [M(CO)_3L_2PF_6]_{ip} + [M(CO)_3L_2X]_{ip}$ and

$$K = \frac{[M(CO)_3L_2X]_{ip}[Bu_4NPF_6]_{ip}}{[Bu_4NX]_{ip}([M(CO)_3L_2^+]_T - [M(CO)_3L_2X]_{ip})} \quad (1)$$

$$\frac{-d[M(CO)_3L_2X]}{dt} = k[M(CO)_3L_2X]_{ip} = \frac{kK[M(CO)_3L_2^+]_T[Bu_4NX]_{ip}}{([Bu_4NPF_6]_{ip} + [Bu_4NX]_{ip}K)} \quad (2)$$

Since

(24) (a) Fuoss, R. M. *J. Am. Chem. Soc.* **1958**, *80*, 5059. (b) Eigen, M. *Z. Elektrochem.* **1960**, *64*, 115.
(25) Pearson, R. G.; Ellgen, P. *Inorg. Chem.* **1967**, *6*, 1379.
(26) Nielson, R. M.; Wherland, S. *Inorg. Chem.* **1984**, *23*, 1338.

$$\frac{-d[M(CO)_3L_2X]_{ip}}{dt} = k_{obs}[M(CO)_3L_2^+]_T \quad (3)$$

comparing (2) and (3)

$$k_{obs} = \frac{kK[Bu_4NX]_{ip}}{[Bu_4PF_6]_{ip} + [Bu_4NX]_{ip}K} \quad (4)$$

then yields

$$\frac{1}{k_{obs}} = \frac{[Bu_4NPF_6]_{ip}}{kK[Bu_4NX]_{ip}} + \frac{1}{k} \quad (5)$$

A plot of $1/k_{obs}$ vs $[Bu_4NPF_6]_{ip}/[Bu_4NX]_{ip}$ (Figure 6) shows excellent agreement with the proposed mechanism. The results obtained from the linear least-squares fitting to (5) are listed in Table VIII. The near-unity values obtained for K from this analysis offer further support for its correctness. One would expect little selectivity in the cation–anion pairing among the various ion pairs.

In the absence of $[Bu_4N]PF_6$ and with an excess amount of $[Bu_4N]X$ in the solution, e.g., $[Bu_4NPF_6]_{ip} = 0$ and $[M(CO)_3L_2X]_{ip} \approx [M(CO)_3L_2^+]_T$, (4) simplifies to $k_{obs} = k$. Therefore, the observed rate constant k_{obs} is independent of the concentration of $[Bu_4N]X$ as long as there is enough $[Bu_4N]X$ in solution to push the preequilibrium step in Scheme III to the right.

Activation Parameters. The temperature-dependent data on reaction rates, k, were fitted to the Eyring equation (Figure 7). Derived activation parameters are listed in Table IX. The low values of $\Delta H^\ddagger$ fall within the range 12–20 kcal mol^{-1} and suggest an internal associative interchange mechanism for decay of $[M(CO)_3L_2X]_{ip}$. Although the relative rates show little change on descending the metal triad, the activation enthalpies decrease on progressing from Fe to Os. This would be consistent with stronger bonding to X^- in the 19-electron transition state as the metal becomes more sterically accessible in the order Fe < Ru ≈ Os. The large difference in $\Delta H^\ddagger$ between Ru and Os of similar size must be attributed to electronic effects. Third-row metals generally form stronger bonds to ligands, which is thought to be the reason[4] why dissociative reactions of 18-electron Ru complexes are much faster than those of Os. A significantly smaller $\Delta H^\ddagger$ for Os indicates a strong Os–X bond in the 19-electron transition state. This could also explain the loss of entropy in the transition state, which should be most ordered for Os.

Conclusions

There are several findings in this study, which may be of broader significance. For associative ligand substitution in a charged complex, $[ML_n][Y]$, in a low dielectric constant solvent like CH_2Cl_2, nucleophilic substitution of L by a charged nucleophile X^- may proceed entirely through ion-paired species according to Scheme IV. In general one expects that $K \approx 1$ and k, which is a first-order rate, represents an internal nucleophilic displacement rate within the ion-paired species. When the total $[X]/[Y]$ ratio is large, the reaction appears zero order in $[Bu_4N][X]$, but when this ratio is small, a linear dependence is obtained. The more general case follows (5).

Scheme IV

$$\{[ML_n][Y]\}_{ip} + \{[Bu_4N][X]\}_{ip} \overset{K}{\rightleftharpoons} \{[ML_n][X]\}_{ip} + \{[Bu_4N][Y]\}_{ip}$$

$$\{[ML_n][X]\}_{ip} \xrightarrow{k} \text{products}$$

In a system such as in Scheme IV the reactivity of $[X^-]_{free}$ has little kinetic significance, because in order to react with $\{[ML_n][Y]\}_{ip}$ it first must form $\{[ML_n][X]\}_{ip}$. Presumably the reaction between the small amount of $[ML_n^+]_{free}$ and $[X^-]_{free}$ also produces the same species. Therefore, k may be common to all possible reaction paths for a given nucleophile and represents the limiting step for all species. The data allow us to rule out mechanisms that involve the attack of $[X^-]_{free}$ on $[M(CO)_3L_2PF_6]_{ip}$ or $[M(CO)_3L_2X]_{ip}$. However, it does not rule out the possible direct attack of $[X^-]_{free}$ on $[M(CO)_3L_2^+]_{free}$, since $[X^-]_{free}[M(CO)_3L_2^+]_{free} = K_d[M(CO)_3L_2X]$. We do not favor this possibility for several reasons. Earlier work on substitution reactions of transition-metal complexes such as Pt(II)[27] have established that pyridine is a better nucleophile than Cl^-. Our previous work[3b] found that the second-order rate constant (k_2) for the reaction between $Fe(CO)_3(PCy_3)_2^+$ and pyridine is 1.5×10^{-4} s^{-1} M^{-1}. Using the K_d of 1.7×10^{-4} for $\{[Fe(CO)_3(PCy_3)_2][PF_6]\}_{ip}$, we

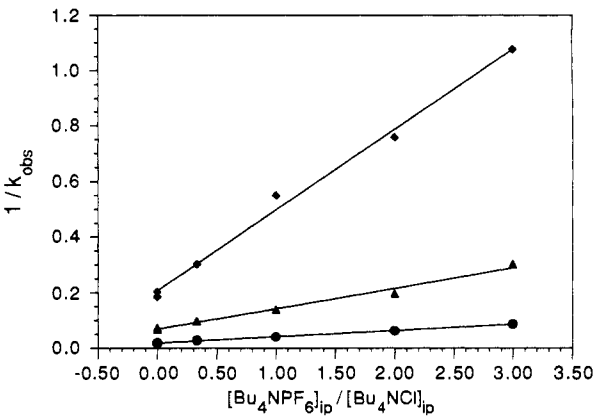

Figure 6. $1/k_{obs}$ as a function of $[Bu_4NPF_6]_{ip}/[Bu_4NCl]_{ip}$ for the reaction between $M(CO)_3(PCy_3)_2^+$ and $[Bu_4N]Cl$: (●) M = Ru; (▲) M = Fe; (◆) M = Os.

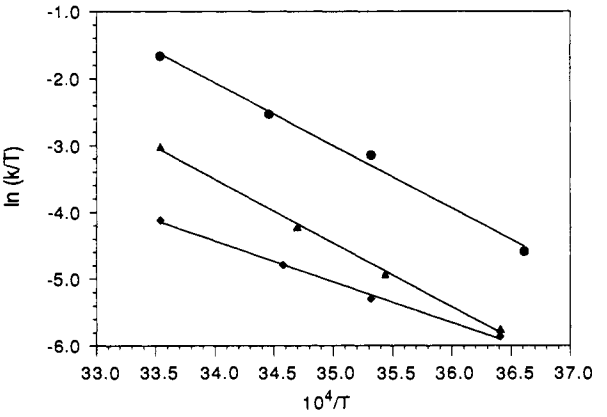

Figure 7. Eyring plots for the reaction between $M(CO)_3(PCy_3)_2^+$ and $[Bu_4N]Cl$: (●) M = Ru; (▲) M = Fe; (◆) M = Os.

Table VIII. First-Order Rate Constants for Decay of the $[M(CO)_3(PCy_3)_2X]_{ip}$ and Equilibrium Constants for Ion Pair Exchange Derived from Fitting (5) for the Reaction between $M(CO)_3(PCy_3)_2^+$ and $[Bu_4N]X$ at 25.0 °C

radical	halide	k, s^{-1}	K
$Fe(CO)_3(PCy_3)_2^+$	$[Bu_4N]Cl$	15 ± 3	0.9 ± 0.2
$Fe(CO)_3(PCy_3)_2^+$	$[Bu_4N]Br$	3.3 ± 0.1	0.98 ± 0.03
$Ru(CO)_3(PCy_3)_2^+$	$[Bu_4N]Cl$	56 ± 5	0.79 ± 0.07
$Ru(CO)_3(PCy_3)_2^+$	$[Bu_4N]Br$	5.5 ± 0.5	1.02 ± 0.05
$Os(CO)_3(PCy_3)_2^+$	$[Bu_4N]Cl$	4.8 ± 0.9	0.7 ± 0.1
$Os(CO)_3(PCy_3)_2^+$	$[Bu_4N]Br$	4.4 ± 0.7	0.9 ± 0.1

Table IX. Activation Parameters for the Reaction between $M(CO)_3(PCy_3)_2^+$ and Bu_4NCl in CH_2Cl_2[a]

complex	$\Delta H^\ddagger$, kcal mol^{-1}	$\Delta S^\ddagger$, cal mol^{-1} K^{-1}
M = Fe	19.7 (±0.9)	10 (±3)
M = Ru	18.7 (±1.6)	12 (±5)
M = Os	12.1 (±0.7)	−14 (±3)

[a] Derived from the temperature dependence of the first-order rate constants (k) for $[M(CO)_3(PCy_3)_2X]_{ip}$.

(27) (a) Gray, H. B. *J. Am. Chem. Soc.* **1962**, *84*, 1548. (b) Banerjea, D.; Basolo, F.; Pearson, R. G. *J. Am. Chem. Soc.* **1957**, *79*, 4055.

estimate that k_2 for the $[Fe(CO)_3(PCy_3)_2^+]_{free}$ pathway is at most 4.5×10^{-4} M^{-1} s^{-1}. A k_2 of 1.5×10^5 M^{-1} s^{-1} for the rate of the direct reaction between $[Fe(CO)_3(PCy_3)_2^+]_{free}$ and $[Cl^-]_{free}$ is required on the basis of our present experimental data and the estimated K_d of 10^{-4}. This requires a nucleophilicity 10^8 greater for Cl^- than for pyridine. Rather than attribute Cl^- a tremendously enhanced nucleophilicity it seems more reasonable to attribute the difference to the special role ion pairing may play in enhancing the local concentration of Cl^- for nucleophilic attack at the cationic metal center.

In the context of periodic trends for the reactivity of organometallic radicals, the data suggest a greatly reduced effect in comparison to analogous 18-electron complexes. For chloride as nucleophile the reactivity order at 25 °C Os (1) < Fe (2.9) < Ru (11.7) shows an enhanced rate for the second-row metal, but much reduced from the 10^7–10^8 increase in lability of Ru for the related 18-electron systems discussed in the Introduction. For bromide as nucleophile there is essentially no discrimination in reactivity between Fe, Ru, and Os. This cannot be simply attributed to the reactivity–selectivity principle, because the rates observed are not terribly fast. There are a few other examples in the literature, which suggest periodic trends are attenuated in 17-electron systems. The reasons behind this may be the importance of bond formation to the metal in the 19-electron intermediate or transition state postulated in such reactions. For 18-electron iron, ruthenium, and osmium carbonyls, a strong metal–carbonyl bond needs to be broken in the dissociative transition state. One postulate is the relative activation energies parallel relative bond strengths, which are weakest for second-row metals. In 17-electron systems, where the mechanism changes to an associative process, several factors should influence activation barriers (steric effects, entering and leaving group effects). An analysis of the activation parameters suggest that ΔH^* trends, related to stabilization of the 19-electron species by metal–nucleophile bonding, favor the third-row metals. Indeed, there are some parallels to the behavior of (mesitylene)$W(CO)_3^+$ and (mesitylene)$Cr(CO)_3^+$. The tungsten complex exhibits an enhanced reactivity in comparison to chromium.[28] This suggests that oxidation to a 17-electron complex is an excellent way to turn on the substitution reactivity of the sluggish third-row 18-electron metal complexes.

Acknowledgment. This work was supported by a National Science Foundation grant (CHE-88-15958). We thank Prof. W. L. Gladfelter for a preprint of ref 21.

Supplementary Material Available: Tables of pseudo-first-order rate constants (k_{obs}), first-order rate constants (k), and equilibrium constants for ion pair exchange (K) determined for Scheme III as a function of temperature for the reaction between $[M(CO)_3(PCy_3)_2]PF_6$ and $[Bu_4N]X$ (M = Fe, Ru, Os; X = Cl, Br) (8 pages). Ordering information is given on any current masthead page.

(28) Zhang, Y.; Gosser, D. K.; Rieger, P. H.; Sweigart, D. A. *J. Am. Chem. Soc.* **1991**, *113*, 4062.

The Deceptively Simple Thermolysis of Trivalent Permethyltitanocene Derivatives $(\eta^5\text{-}C_5Me_5)_2TiR$. Formation of a Tetramethylfulvene Titanium Compound $(\eta^6\text{-}C_5Me_4CH_2)(\eta^5\text{-}C_5Me_5)Ti$ and RH, Catalyzed by Permethyltitanocene Hydride, $(\eta^5\text{-}C_5Me_5)_2TiH$

Gerrit A. Luinstra and Jan H. Teuben*

Contribution from the Groningen Center of Catalysis and Synthesis, Department of Chemistry, University of Groningen, Nijenborg 16, 9747 AG Groningen, The Netherlands.
Received August 26, 1991

Abstract: The complexes Cp^*_2TiR ($Cp^* = \eta^5\text{-}C_5Me_5$; R = Me, Et, *n*-Pr, C_2H_3, CH_2CMe_3, Ph) undergo thermolysis to yield the fulvene complex Cp*FvTi (Fv = $\eta^6\text{-}C_5Me_4CH_2$) and RH. Kinetic measurements and deuterium labeling studies show that the decomposition is catalyzed by Cp^*_2TiH, which is formed either by β-hydrogen elimination from a titanium alkyl $Cp^*_2TiCH_2CH_2R$ at low temperature or by hydrogenolysis of Cp^*_2TiR or Cp*FvTi, using dihydrogen eliminated from Cp*FvTi at elevated temperatures. Permethyltitanocene is not an intermediate. The rate of the catalyzed decomposition of $Cp^*_2TiCH_2CMe_3$ is linear in $[Cp^*_2TiH]$. For Cp^*_2TiMe it is proportional to $[Cp^*_2TiH]$ and $[Cp^*_2TiMe]$ and inversely proportional to the starting concentration of Cp^*_2TiMe. This is explained in a kinetic scheme, where H_2, eliminated from Cp^*_2TiH to give Cp*FvTi, reacts with Cp^*_2TiR to regenerate Cp^*_2TiH and liberate RH. The model is supported by the reaction of $(Cp^*\text{-}d_{15})_2TiD$ and $Cp^*_2TiCH_2CMe_3$ yielding Cp^*_2TiD and (Cp*FvTi-d_{29}).

Introduction

The activation of C–H bonds of inert hydrocarbons has been a major topic in contemporary organometallic chemistry.[1] It is generally recognized that C–H bonds can be activated either by oxidative addition to an electron-rich metal center or by a nonoxidative pathway at a strongly electrophilic metal center.[2] The latter is typical for the strongly Lewis acidic d^0 transition metal and lanthanide compounds.[3] Intermediates may involve cu-

(1) (a) Shilov, A. E. *Activation of Saturated Hydrocarbons by Transition Metal Complexes*; D. Reidel: Dordrecht, 1984; Chapter 1 and references therein. (b) Crabtree, R. H. *Chem. Rev.* **1985**, *85*, 245.

(2) See: Ryabov, A. D. *Chem. Rev.* **1990**, *90*, 403.

(3) See: (a) Watson, P. L.; Parshall, G. W. *Acc. Chem. Res.* **1985**, *18*, 51 and references therein. (b) Thompson, M. E.; Bercaw, J. E. *Pure Appl. Chem.* **1984**, *56*, 1. (c) Parkin, G.; Bunel, E.; Burger, B. J.; Trimmer, M. S.; Van Asselt, A.; Bercaw, J. E. *J. Mol. Catal.* **1987**, *41*, 21. (d) Jeske, G.; Lauke, H.; Mauermann, H.; Swepston, P. N.; Schumann, H.; Marks, T. J. *J. Am. Chem. Soc.* **1985**, *107*, 8091. (e) Hlatky, G. G.; Turner, H. W.; Eckman, R. R. *J. Am. Chem. Soc.* **1989**, *111*, 2728. (f) Jordan, R. F.; Guram, A. S. *Organometallics* **1990**, *9*, 2116. (g) Heeres, H. J.; Heeres, A.; Teuben, J. H. *Organometallics* **1990**, *9*, 1508.

0002-7863/92/1514-3361$03.00/0